

EXCITON-CAPTURE AND AUGER-RECOMBINATION RATES
 OF BOUND MULTIEXCITON COMPLEXES IN SILICON

H. Nakayama, T. Nishino and Y. Hamakawa

Faculty of Engineering Science
 Osaka University
 Toyonaka, Osaka
 Japan

The formation and decay processes of bound multi-exciton complexes in Si have been investigated with systematic measurements for the excitation-level and impurity-content dependences of their luminescence intensity. From the analysis of data the exciton-capture and Auger-recombination rates of P, B and Li bound multiexciton complexes have been obtained for the first time, the results indicating a close relation to the "shell structure".

I. Introduction

In the recent few years extensive investigations have been concentrated so as to clarify the origin of satellite line series at the low-energy side of the bound-exciton (BE) luminescence line in lightly-doped Si [1,2]. These lines are presently attributed to the radiative recombination of an electron-hole pair localized in bound multiexciton complexes (BMEC). Especially, the shell model (SM) [3] which postulates the electronic structure of BMEC well explain experimental data including Zeeman and uniaxial-stress effect data [2]. On the other hand, dynamical behaviors of the BMEC system, which are closely related to the nucleation problem of electron-hole droplets [4], have remained so far unknown for the most part in both experimental and theoretical aspects. Recently, we have found that the exciton-capture (EC) and Auger-recombination (AR) rates of BMEC can be determined by the analysis of BMEC-luminescence intensity based on kinetic equations describing the formation and decay processes of the whole system including free exciton (FE), BE and BMEC. In this paper we present the data for EC and AR rates of BMEC in Si:P, Si:Li and Si:B, with emphasis on the relation to the shell structure of BMEC for these impurity species.

II. A method of determining the EC and AR rates of BMEC

Kinetic equations which describe dynamical behaviors of the whole system including FE, BE and BMEC are written as follows [5];

$$\frac{\partial n_m}{\partial t} = C_{m-1} N n_{m-1} - C_m N n_m + W_{m+2} n_{m+2} - W_m n_m, \quad (1)$$

$$\frac{\partial N}{\partial t} = g - W_f N - \sum_{m=0}^{\infty} C_m N n_m + \sum_{m=2}^{\infty} W_m n_m, \quad (2)$$

where n_m is the density of the m -th BMEC and N is that of FE. C_m and W_m are the EC and AR rates of the m -th BMEC, respectively. g and W_f are the FE-generation rate and the recombination rate. In this formula, we consider EC and AR processes as principal ones which

determine the density of FE, BE and BMEC, and other dynamical processes such as thermal dissociation process of BE and BMEC are neglected. This approximation is verified in the temperature range around 4.2 K where the AR process is the dominant decay channel of these BMEC states [6]. We define a luminescence-intensity ratio, described as R_m , of the m -th BMEC relative to the $(m+1)$ -th BMEC. From the solution in the steady-state condition [5] of the above mentioned coupled eqs. (1) and (2), R_m is given as a function of the excitation intensity I_e by

$$R_m = \frac{W_{r,m}}{W_{r,m+1}} \frac{n_m}{n_{m+1}} = \frac{W_{r,m}}{W_{r,m+1}} \left\{ \frac{W_{m+1}}{C_m} \frac{1}{K\tau_{\text{eff}}} \frac{1}{I_e} + \frac{C_{m+1}}{C_m} \right\}, \quad (3)$$

where $W_{r,m}$ is the radiative-recombination rate of the m -th BMEC and K is a proportional constant in the form of $g = KI_e$. τ_{eff} is the effective recombination lifetime of FE. In the analysis of BMEC-luminescence intensity, so-called α line-series in the no-phonon spectral region are taken into account for P. And principal BMEC lines in the TO-phonon region are used for B and Li. Here, the radiative-recombination rate $W_{r,m}$ is assumed to be proportional to the product of the numbers of electron and hole in the specific shell involved in the transition [3]. From eq. (3) it is found that the luminescence-intensity ratio R_m is a linear function of the inverse excitation intensity $1/I_e$, for τ_{eff} is nearly independent of I_e [5]. And hence, the EC and AR rates in the form of their ratio can be obtained from R_m vs $1/I_e$ plots by using the following relations;

$$\frac{C_{m+1}}{C_m} = \frac{W_{r,m+1}}{W_{r,m}} R_m (1/I_e=0), \quad (4)$$

$$\frac{W_{m+1}}{W_m} = \frac{W_{r,m-1} W_{r,m+1}}{(W_{r,m})^2} \frac{C_m}{C_{m-1}} \frac{a_m(N_I)}{a_{m-1}(N_I)}, \quad (5)$$

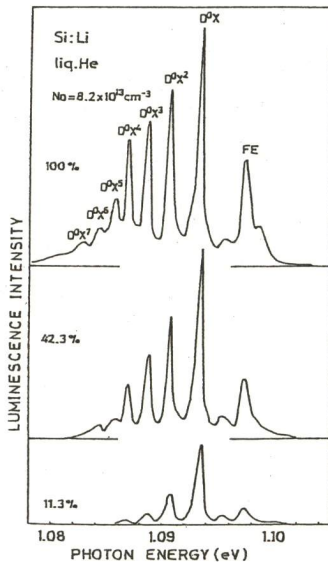


Fig.1 Exciton-luminescence spectra of Si:Li in the TO-phonon region

where $a_m(N_I)$ is the slope of R_m vs $1/I_e$ plots for a sample with the impurity concentration of N_I . Furthermore, the value of C_0 , which is the EC rate at a neutral impurity center, can be also determined from an analysis of the excitation-level dependence data of BE and FE [7].

III. Results and Discussion

Figure 1 shows the excitation-level dependence of the luminescence spectra of Si:Li. It should be noted in the figure that the intensity of higher-order BMEC decreases more rapidly than lower-order BMEC when the excitation power decreases as is expected from eq. (3). We have measured systematically the excitation-level dependence for P-, Li- and B-doped Si with the doping range of $10^{12} \sim 10^{15} \text{ cm}^{-3}$. Figure 2 shows typical results for the luminescence-intensity ratio R_m ($m=1, 2$ and 3) as a function of $1/I_e$ for Si:Li. Essential features observed for these plots are as follows; (1) Data points of R_m are well on straight lines for all the samples.

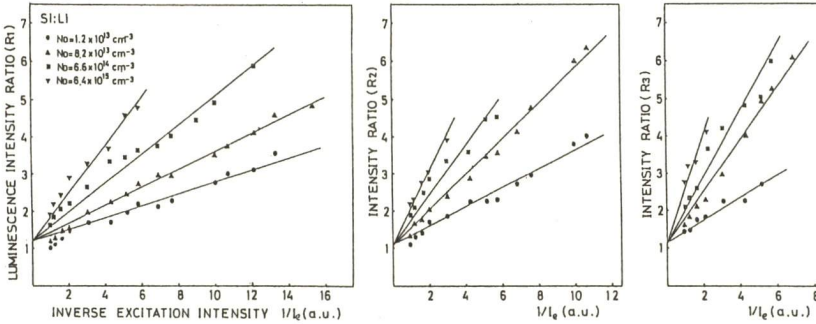


Fig.2 Plots of the luminescence-intensity ratio R_m ($m=1, 2$ and 3) of the m -th BMEC relative to the $(m+1)$ -th BMEC as a function of inverse excitation intensity $1/I_e$

(2) The slopes of the lines become larger with increasing impurity concentration. (3) All the straight lines have the same intersection at $1/I_e=0$. These behaviors have been also observed for Si:P and Si:B, which are consistent with the theoretical prediction from eq. (3). From these data we obtain AR and EC rates of BMEC by the use of eqs. (4) and (5). Figure 3 shows the plots of the AR rates of BMEC normalized by that of BE. As is well known that the AR process which involves three particles, that is two electrons and one hole (eeh-process) or one electron and two holes (ehh-process), is characterized by its carrier-density dependence of the rate; n^2p -dependence for eeh-process and np^2 -dependence for ehh-process, where n and p are the electron and hole density. We have also calculated the AR rates of donor-BMEC using $W_m = A(n_{1,m})^2 p_{1,m}$, where A is a proportional constant and $n_{1,m}$ and $p_{1,m}$ are the "local density" of electrons and holes in the m -th BMEC defined as $n_{1,m} = (m+1)[(4\pi/3)(r_{e,m})^3]^{-1}$ and $p_{1,m} = m[(4\pi/3)(r_{h,m})^3]^{-1}$, where $r_{e,m}$ and $r_{h,m}$ are Bohr radius of electron and hole in the m -th BMEC. The values of $r_{e,m}$ and $r_{h,m}$ have been recently estimated by Wünsche et al. [8]. The calculated results of AR rates are plotted in Fig. 3. As is shown in the figure, the variation of AR rates of P-BMEC

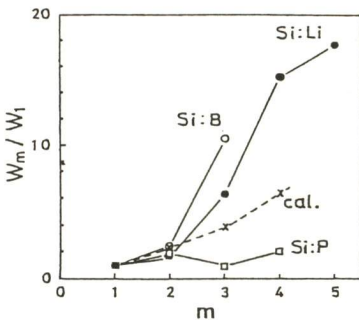


Fig.3 Plots of Auger-recombination rates as a function of the order m of BMEC, where $m=1$ means BE: Dotted line shows calculated data

with the order m of BMEC is small as compared with those of Li- and B-BMEC and calculated values. For P-BMEC, as is expected by SM, two electrons in the first Γ_1 shell are highly localized in the central-cell region of an impurity center compared with remaining electrons in the next $\Gamma_{3,5}$ shell, and hence two electrons in the Γ_1 shell effectively contribute to the AR process. This makes the variation of the AR rate with the order m of BMEC to be small. On the contrary, in the case of Li all the electrons in the ten-fold $\Gamma_{3,5}$ inner shell contribute equally to the AR process and therefore the rates strongly depend on the total numbers of electron and hole. The difference between the obtained AR rates for Li and calculated values is probably due to the fact that the change of the $r_{e,m}$ and $r_{h,m}$ with the order m is smaller for Li than those from calculations by Wünsche et al., where shell structures have not been considered. As can be seen in Fig. 3, the behaviors of AR rates of B-BMEC

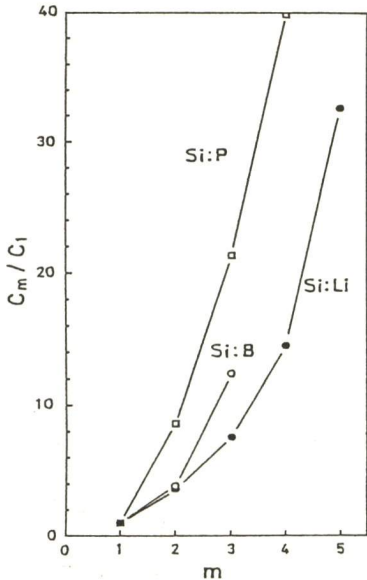


Fig.4 Plots of exciton-capture rates as a function of the order m of BMEC

having the highly degenerate inner shell like Li are similar to those of Li-BMEC.

The EC rates of P-, Li- and B-BMEC obtained from the method described above are shown in Fig.4. The clear difference in the dependence of the EC rates on the order m among these impurity species is also observed. Contrary to the behaviors of AR rates, the EC rates of P-BMEC show a strong dependence on the order m compared with B- and Li-BMEC. In the EC process of BMEC two types of processes can be considered; the first process in which an exciton is captured into the inner shell of the $(m-1)$ -th BMEC leaving the m -th BMEC in the ground state and the second process in which an exciton is captured into the outer shell of the $(m-1)$ -th BMEC leaving the m -th BMEC in the excited state. The latter process is similar to the cascade capture process of charge carriers at an ionized impurity center. Our results of theoretical calculation for a phonon-assisted EC rate show that the latter process is more effective than the former one because in the latter process momentum transferred from FE to phonon is smaller. The detailed results will be reported elsewhere.

It should be also noted that P-BMEC has the highly degenerate (ten-fold) outer

electron $\Gamma_{3,5}$ shell and Li-BMEC has the doubly degenerate outer electron Γ_1 shell. This difference of the degeneracy of excited shell between P and Li is considered to be closely related to the difference in the behaviors of EC rates observed in Fig.4.

This work was supported in part by the Grant-in-Aid from the Ministry of Education, Science and Culture. The authors wish to thank Mr. K. Ohnishi for his valuable discussion and technical assistance. One of us (T. N.) acknowledges the financial support by the Nishina Memorial Foundation.

References

- 1) R. Sauer: Proc. Int. Conf. Phys. Semicond., Stuttgart (1974) p.42.
- 2) M.L.W. Thewalt: Proc. Int. Conf. Phys. Semicond., Edinburgh (1978) p.605.
- 3) G. Kirczenow: Canad. J. Phys. 55 (1977) 1787.
- 4) R.N. Silver: Phys. Rev. B 11 (1975) 1569.
- 5) H. Nakayama, K. Ohnishi, H. Sawada, T. Nishino and Y. Hamakawa: J. Phys. Soc. Japan 46 (1979) 553.
- 6) S.A. Lyon, D.L. Smith and T.C. McGill: Phys. Rev. Letters 41 (1978) 56.
- 7) H. Nakayama, T. Nishino and Y. Hamakawa: Jpn J. Appl. Phys. 19 (1980) 501.
- 8) H.-J. Wunsche, K. Henneberger and V.E. Kartsiev: Phys. Status Solidi (b) 86 (1978) 505.